연료전지 시스템을 위한 풀-브리지 소프트 위상 천이 PWM DC-DC 컨버터

(Full-bridge Soft-Switching PS-PWM DC-DC Converter for Fuel Cell Generation System)

*문상필, 서기영, 이현우, M.Nakaoko, 신휘범**

(*S. P. Mun, K. Y. Suh, H. W. Lee, S. K. Kwon, M. Nakaoko, H. B. Shin*)

경남대학교, 경상대학교

(Kyung-nam University, Gyeong-Sang National University*)

Abstract

In this paper, a new a new full-bridge soft-switching phase shift PWM DC-DC Converter has been proposed, which is suitable for fuel cell based power generation system. The proposed converter has outstanding advantage over the conventional DC-DC converter with respect to high efficiency, high power density, and high component utilization. In special, the proposed converter has predominant high boosting output voltage and high efficiency characteristics under the inherently severs low output voltage of the fuel cell through the overall load conditions. Moreover, the developed c onverter has been experimentally tested with the help of a fuel cell simulator, and can generate the V-I characteristics of proton exchange membrane(PEM)fuel cell, so that the performance of the proposed converter could be effectively examined and the validity of the converter could be verified.

1. INRODUCTION

In recent, Fuel Cells(FCs)are regarded as a good alternative renewable energy source, which can solve the pacing problems, such as exhausting fossil energy and severe environmental pollution. However, the FC should overcome its inherent restrictions, such as very low output voltage, large voltage variation and slow dynamic response according to the load variations, and low fuel efficiency due to the high ripple current. In order to effectively apply the FC in the real world, the FC is generally integrated with Power Conditioner System(PCS), which consist of DC-DC converter, a bi-directional DC-DC converter, a DC-AC inverter.

The compared with the conventional PCS for switched-mode power supplies, UPSs, and adjustable speed motor drives, the PCS for the FC (FC-PCS) should be differently implemented in topological and control point of views due to the complicated FC's physical problems. Until now many researchers have paid their attention to the development of the FC-PCS and several topologies have been reported. These topologies are mainly about dc-dc converters, which are difficult to design and control because that they are directly connected to the FC stack at the first stage. Although they meet the general requirements of conventional boost DC-DC converters, they are based on voltage-source configuration and they have no dynamic verification with the actual FC V-I characteristics, which make them apart from using in the actual FC applications. Also, compared with the other applications, in the FC applications, voltage -source converter configurations may not be optimal one due to the severe tipple current characteristic of the FC. In order to handle the ripple current, a large and many number of electrolyte capacitor are essentially required, resulting in increase of the overall system size and manufacturing cost.

Moreover, in voltage-fed converters, high winding ratio between primary and secondary sides of the high frequency transformer is necessary because the boosting action is only performed by the winding ratio and also it cause the snubber be enlarged to handle the surge at turn-off switching instants.

In this paper, a new Full-bridge Soft-Switching PS-PWM DC -DC Converter for fuel-cell generation system has been proposed, which solve the problems of the conventional converter. In special, the proposed converter has predominant high boosting output voltage and high efficiency characteristics under the inherently severs low output voltage of the fuel cell through the overall load conditions. Moreover, the developed converter has been experimentally tested with the help of a fuel cell simulator, and can generate the V-I characteristics of Polymer Electrolyte Membrane Fuel Cell (PEMFC), so that the performance of the proposed converter could be effectively examined and the validity of the converter could be verified.

2. Analysis and Operational Principles of the Proposed Converter

Fig. 1 shows the block diagram of DC-DC boost converter scheme. In the figure DC-DC converter are combined with fuel cells, and bi-directional buck-boost converter is combined with a super -capacitor. The control scheme is combined of one voltage control loops and two independent current control loops and the DC-bus voltage is controlled by a PI controller to generate the system current command. Power available signal from the fuel cell indicates the available power from the fuel cell at the moment and thereby available current command is calculated.

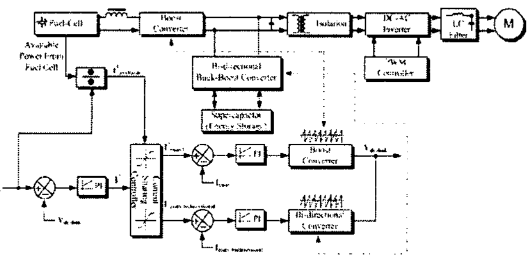

Fig. 1 Block diagram of the system control.

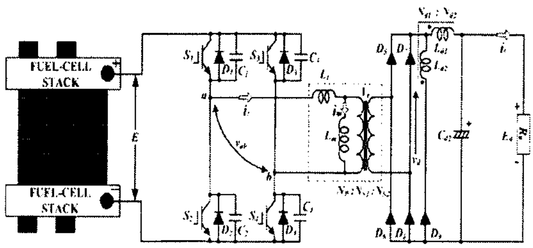

Fig. 2 Proposed full-bridge soft-switching PS-PWM DC-DC converter for fuel-cell generation system

Fig. 2 shows a schematic circuit configuration of the proposed soft-switching full-bridge PS-PWM DC-DC converter with the tapped inductor filter L_{d1}/L_{d2} and freewheeling diode D_9 in its output stage. The lossless snubber capacitors C_1 and C_2 connected in parallel with leading bridge-leg active power semiconductor switching devices(switches)S_1 and S_2 are used to obtain ZVS operation by reducing dv/dt across these switches. The lagging bridge-leg switches S_3 and S_4 operate with ZCS at a turn-on due to the effect of an inductance L_l to suppress di/dt.

This inductance L_l can be substituted by leakage inductance of the high frequency transformer Tr. In addition, the tapped inductor filter L_{d1}/L_{d2} with connected freewheeling diode D_9 are used to obtain ZCS for switches S_3 and S_4 at a turn-off as well as to minimize circulating current during the freewheeling interval.

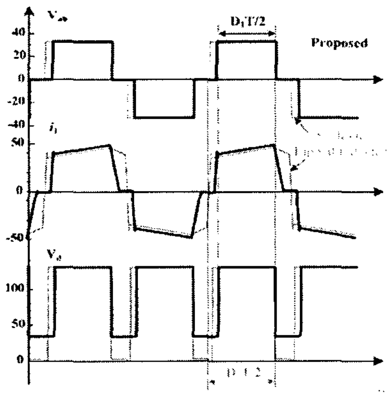

Fig. 3 Operation waveforms of PS-PWM DC-DC converter.

In the situation of a power shortage or instantaneous overload current sharing controller calculates the appropriate current command values for each converter and sends it to them. Fig. 3 shows the operation waveforms of the proposed PS-PWM DC-DC power converter with the tapped inductor filter compared to the conventional ZVS PS-PWM DC-DC power converter without tapped inductor.

In case of the proposed DC-DC converter to achieve the same power in the output with the conventional DC-DC converter, the duty cycle D_1 ($D=t_{on}/T$) is smaller than duty cycle D_2 of the conventional converter. It means that to achieve the same power in the output the DC source must be connected to the output through DC-DC converter circuit shorter time and it is prove that the circulating current can be reduced. The operation during the next half-cycle is symmetrical with the mentioned above half-cycle and does not shown. As described above the switches S_1 and S_2 are turned on and turned off with ZVS, while the switches S_3 and S_4 operate with ZCS at turn-on and turn-off. The circulating current during the freewheeling interval t_0-t_4 is substantially lowered. As was shown above, the tapped inductor L_{d1}/L_{d2} in the proposed soft-switching PS-PWM DC-DC power converter operates as a smoothing inductor and also makes that the rectified output voltage v_d is clamped to the value $v_d=\alpha_L E_0$ during the freewheeling interval. Therefore, the clamped voltage $v_d=\alpha_L E_0$ is applied during the freewheeling interval to the transformer leakage inductance L_l and reset its energy to zero. As result during the freewheeling interval, the output current flows through the additionally connected freewheeling diode D_9.

The using tapped inductor filter L_{d1}/L_{d2} with connected freewhee-ling diode makes possible to reduce the circulating current without using any active switches and theirs driver circuit. Fig. 4 shows the rectified voltage v_d waveform. During a half cycle period, the rectified voltage v_d is expressed as,

$$\begin{cases} v_d = N_L E_0 & \text{for} \quad t_0 < t \le t_4 \\ v_d = \dfrac{E}{N_T} & \text{for} \quad t_4 < t \le t_5 \end{cases} \qquad (4)$$

The output voltage characteristic equation of the proposed DC-DC power converter can be represented by,

$$E_0 = \frac{DE}{\alpha_T\{1-\alpha_L(1-D)\}} - \frac{L_s I_0}{\alpha_T^2 T_h \{1-\alpha_L(1-D)\}^2} \qquad (5)$$

To make the average output voltage E_0 characteristic independent of the output current I_0, and to obtain effective cancellation of the circulating current, the leakage inductance Ls of the high frequency transformer is designed as small as possible.

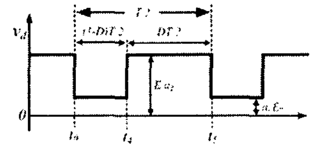

Fig. 4 Operating waveform of rectified voltage v_d.

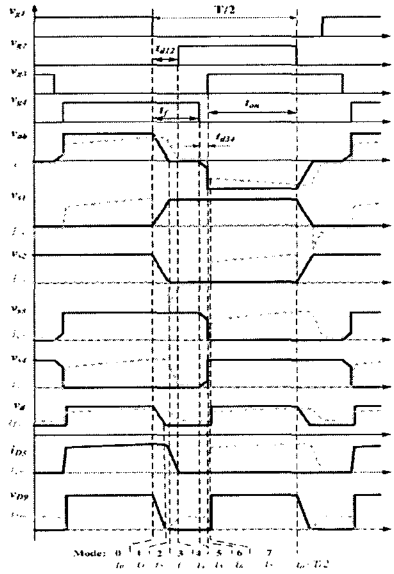

Fig. 5 Operation waveforms of the proposed soft-switching PS-PWM DC-DC converter.

Fig. 5 illustrates switching pulse sequences and theoretical operating voltage and current waveforms of the presented converter at steady state. The switches S_1 and S_2 are driven complementary with the blanking interval t_d. This interval t_d is needed to obtain the ZVS commutation of the switches $S_1$and S_2 at the turn-on instant. The dead time of the switches S_3 and S_4 is designed from consideration of the switching power devices and theoretically does not need for soft-switching operation of these switches. The output voltage of the proposed DC-DC converter is regulated by lagging the gate pulse of the switch $S_4(S_3)$ with respect to the gate pulse of the switch $S_1(S_2)$ and varying by this way an interval t_{on} ($t_{on}=DT/2$) as PS-PWM control with the constant switching frequency $f=1/T$.

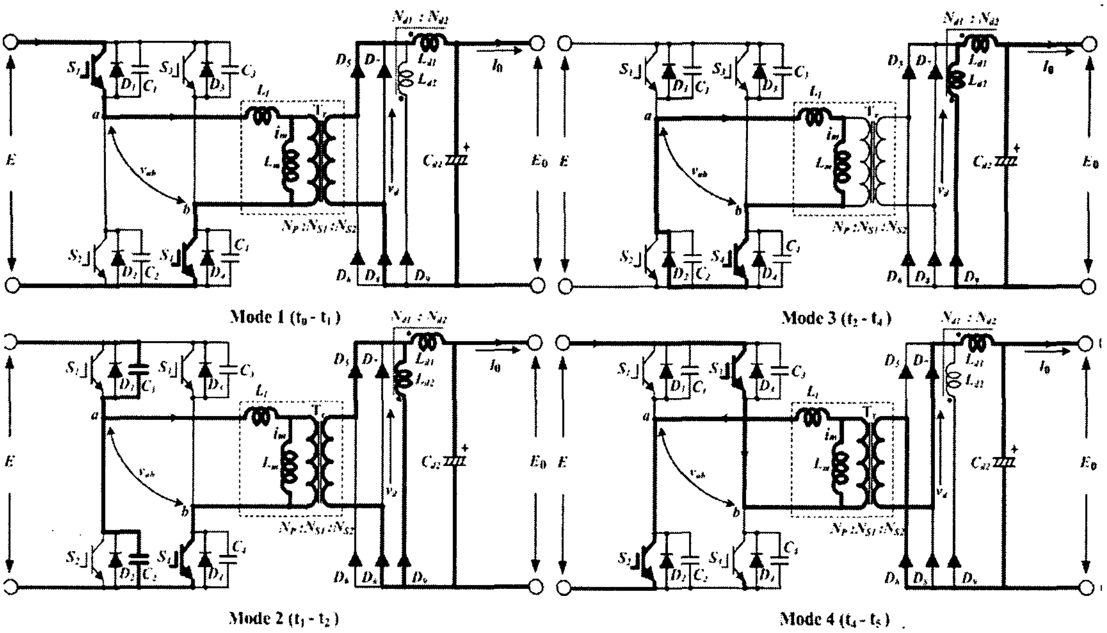

Fig. 6 Equivalent circuits during a half period of steady state operation

Fig. 6 shows the equivalent circuits of the main operation modes during a half cycle. The principle of the proposed soft- switching PS-PWM DC-DC power converter circuit operation in steady-state condition can be described as follows.

Mode 1(t_0, t_1) : Before time t_0, it is consumed, that switches S_1, S_4 and rectifier diodes D_5, D_8 are conducting. The power is transferred through the high frequency transformer Tr from DC voltage source E to the load. The magnetizing current flows through the high frequency transformer magnetizing inductance L_m.

Mode 2(t_1, t_2) : At the instant t_0, the switch S_1 is turned-off with ZVS due to using lossless snubber capacitors C_1 and C_2. The high frequency transformer Tr primary side voltage, the secondary side voltage and the rectified voltage $v_d$go down toward zero. Due to the effect of the tapped inductor L_{d1}/L_{d2} with the freewheeling diode D_9 in the output filter stage, the rectified voltage v_d is clamped to the value $v_d = \alpha_L E_0$, where α_L is the turns ratio of the tapped inductor defined as $\alpha_L = n_2/(n_1+n_2)$; n_1, n_2 are the number of turns of L_{d1} and L_{d2}, respectively. Therefore, the freewheeling diode D_9 starts to conduct when the rectified voltage v_d reaches the value $v_d = \alpha_L E_0$.

Mode 3(t_2, t_4) : After the high frequency transformer primary side voltage v_{ab} reaches zero, the resonance between lossless snubber capacitors C_1, C_2 and leakage inductance L_l forces the body diode of the switch S_2 in forward direction and this diode starts to conduct. At the instant t_2, the pulse signal v_{S2} is applied to the gate of the switch S_2 and the switch S_2 operates with ZVS. The transformer rectified current i_{D5} circulates through the transformer secondary side and rectifiers D_5, D_8, its related current circulates in the primary side, and the magnetizing current flows through magnetizing inductance L_m. The leakage inductance current i_l consists of the transformer primary side current related to rectified current and magnetizing current i_m and circulates through S_4 and S_2. Because the transformer is shorted by the switch S_4 and S_2 in transformer primary side and the voltage $v_d = \alpha_L E_0$ is applied through the rectifiers D_5, D_8 to the leakage inductance L_l from the tapped inductor filter L_{d1}/L_{d2} side. The rectified current in the secondary side and its related current in the primary side start to fall down. The interval, when the rectified current achieves zero, depends on the value of initial value of the rectified current i_{D5}, $v_d = \alpha_L E_0$ and leakage inductance L_l. After the rectified current i_{d5} reaches zero, the whole output current flows through D_9, L_{d2} and L_{d1}. Consequently, the output current reflected to the transformer primary side becomes zero. Only the small magnetizing current of the transformer Tr circulates through S_4 and S_2. This interval ends when the switch S_4 is turned off with ZCS at instant t_3.

Mode 4(t_4, t_5) : At time t_4, the switch S_3 is turned on with ZCS due to the effect of leakage inductance L_l to suppress di/dt. The current in the primary side of the transformer starts to flow through the switch S_2 and S_3. On the other hand, output current flowing through L_{d2} and D_9 decreases and diode D_9 turns off. The energy is being delivered through the switches S_3, S_2, and transformer Tr, and rectifier diodes D_6, D_7. The half cycle of operation ends at instant t_5.

The operation during the next half-cycle is symmetrical with the mentioned above half-cycle and does not shown. As described above the switches S_1 and $S_2$are turned on and turned off with ZVS, while the switches S_3 and S_4 operate with ZCS at turn-on and turn-off. The circulating current during the freewheeling interval t_0-t_4 is substantially lowered.

3. Simulation and Experimental Results

Table 1 shows the design parameters of proposed fuel-cell generation system. Fig. 7 shows its dynamic output characteristics.

When the load current changed from 20[A] to 50[A], the transient response is plotted in Fig. 7. Then, the stack is stabilized to 50[A] and 46[V] after approximately 0.05[s]. Of course, since the electrochemical reaction time of Fuel Cells is short time constant, the transient actually shows how the load reacts to a specific change.

The simulated waveforms of the transformer primary side current i_l, inductor L_{d1} current i_{Ld2}, and rectified voltage v_d are shown at Fig. 8. The design of the tapped inductor L_{d1}/L_{d2} turns ratio α_L is made on the basis of the simulation results under the closed loop control scheme.

Table. 1 Design specifications and circuit parameters.

Fuel-Cell	Input Voltage(Vs)	39 ~ 60[VDC]
	inductor	L = 1[mH]
	Super-capacitor	C_{sup} = 1.66[F]
	Super-inductance	L_{sup} = 500[uH]
	Output capacitor( )	C_{d1} = 250[uF]
DC-DC Converter	MOSFET'S	S_{1a}~S_{2a} / S_1~S_4(2SK3228) V_{DS}=80[V], R_{DS}=0.006, I_{DS}=75[A]
	Diodes	D_0 / D_5~D_9(30JL2C41) V_{RRM}=600[V], I_0=30[A]
	Lossless snubber capacitors	C_1~C_4 = 30[nF]
	Transformer turns ratio	α_T = 1 : 13
	Leakage inductance	L_l = 300[nH]
	Magnetizing inductance	L_m = 70[uH]
	Tapped inductor	L_{d1} = 50[uH], L_{d2} = 13[uH] (Tapped inductor turns ratio α_L = 0.3)
	Output capacitor( )	C_{d2} = 250[uF]
Inverter	MOSFET'S	S_5~S_8(2SK3228) V_{DS}=80[V], R_{DS}=0.006, I_{DS}=75[A]
	Output Power(P_0)	3.0[kW]
	Output Voltage(V_0)	220[VAC]
	Switching Frequency	fs = 4.5[kHz]
	Output inductance	L_0 = 900[uH]
	Output capacitance	C_0 = 20[uF]

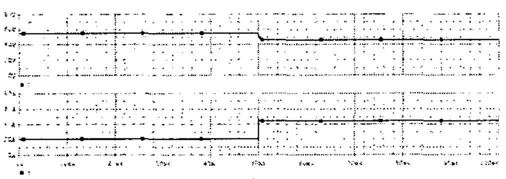

(a) Without time constant

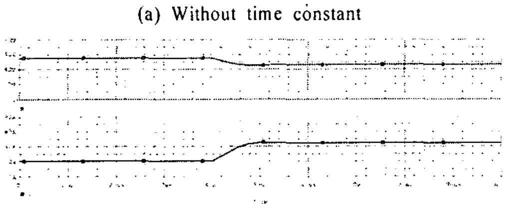

(b) With time constant

Fig. 7 Current voltage transient simulation results of the proposed circuit.

Fig. 9 shows the output characteristics according to the lad variation of FC simulator. Fig. 9(a) shows the voltage-current waveforms when load current changed from 20[A] to 50[A] with not having the time delay function, and Fig. 9(b) represents output characteristics with time delay function.

To verify the operating principle of the proposed soft-switching PS-PWM DC-DC power converter and to evaluate its steady state characteristics, the laboratory level experiment is carried out with a 3[kW] circuit prototype. To achieve high efficiency and high performance of the DC-DC converter the low voltage power MOSFETs are selected as the power active switching devices. The power circuit components parameters are indicated at the Table 1.

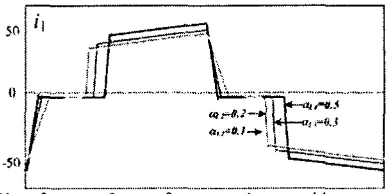

(a) Waveforms of transformer primary side current i_l

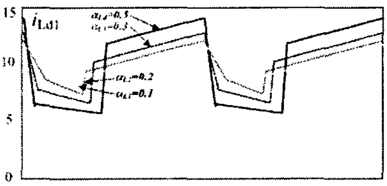

(b) Waveforms of filter inductor L_{d1} current i_{Ld1}

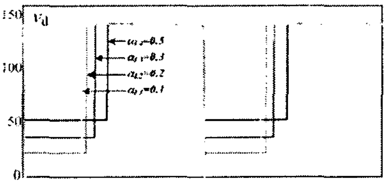

(c) Waveforms of the rectified voltage v_d

Fig. 8 Calculated results under closed loop control scheme.

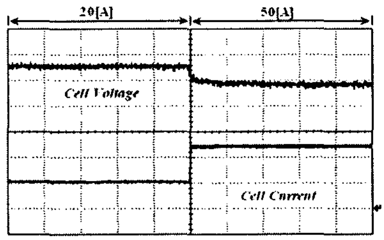

(a) Without time constant(10[V/div], 20[A/div])

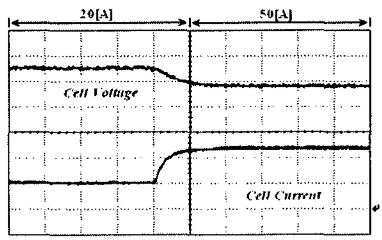

(b) With time constant(10[V/div]. 20[A/div])

Fig. 9 Current voltage transient experimental results of the proposed circuit.(50[ms/div])

Fig. 10(a) and (b) illustrate the measured voltage and current waveforms of the high frequency transformer Tr at 15[%] light and 100[%] full load, respectively. Fig. 11(a). (b) and Fig. 12(a). (b) show the measured voltage and current waveforms and power switches S_2 and S_4 at light and full load, respectively. It is obvious that the circulating current is suppressed during freewheeling interval, and the primary current flows through transformer only when DC source voltage is applied to the transformer. Moreover, the switch $S_2(S_1)$ operates with ZVS, switch $S_4(S_3)$ operate with ZCS at turn-on and turn-off as demonstrated at Fig. 11(a), (b) and Fig. 12(a), (b) at 15[%] light and 100[%] full load. The measured waveforms of the rectified voltage v_d and freewheeling diode D_9 current i_{D9} are presented at Fig. 13.

The output voltage E_0 characteristics of the tested DC-DC power converter as a function of the output current Io under different duty cycle value D are shown at Fig. 13.

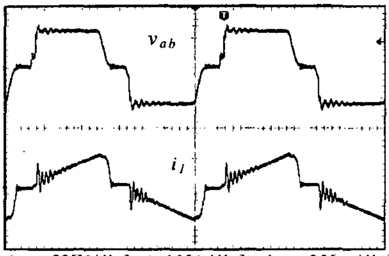

(a) v=50[V/div], i=10[A/div], time=20[μs/div]

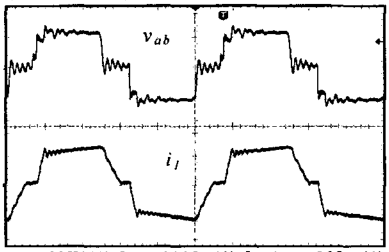

(b) v=50[V/div], i=100[A/div], time=20[μs/div]

Fig. 10 High-frequency transformer Tr voltage v_{ab} and current i_1 waveforms

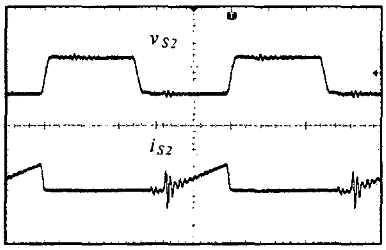

(a) v=50[V/div], i=10[A/div], time=20[μs/div]

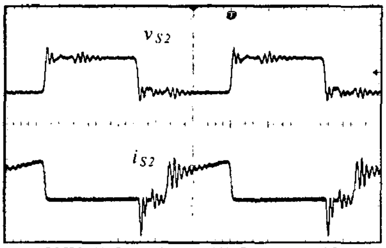

(b) v=50[V/div], i=100[A/div], time=20[μs/div]

Fig. 11 Voltage and current waveforms of switch S_2

The corresponding experimental voltage and current responses of the fuel cell and inverter output terminals at 3.0[kW] resistive load are depicted in Fig. 14. From the experimental results, the favorable regulation performance of the inverter ac output voltage under the fuel cell variant DC voltage can be obtained. By observing the fuel cell current waveform, the current ripple within 120[Hz], which is caused by the ac load component, can be diminished by the utilization of a series of electrolytic capacitors with lower equivalent series resistance(ESR) values.

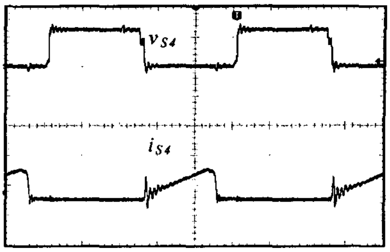

(a) v=50[V/div], i=10[A/div], time=20[μs/div]

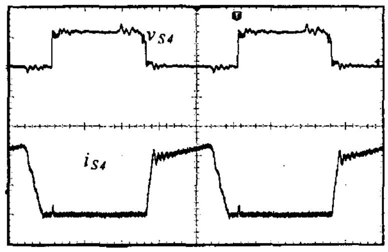

(b) v=50[V/div], i=100[A/div], time=20[μs/div]

Fig. 12 Voltage and current waveforms of switch S_4

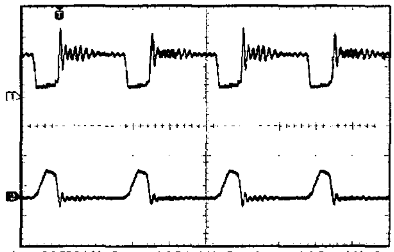
(v=50[V/div], i=10[A/div], time=20[μs/div])

Fig. 13 Measured waveforms of the rectified voltage v_d and freewheeling diode D_9 current i_{D9}

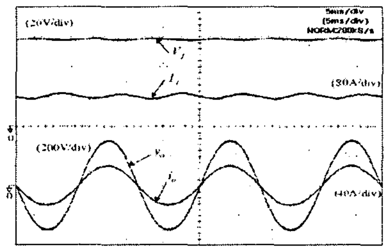

Fig. 14 Experimental voltage and current responses of fuel cell and inverter output terminals at 3.0[kW] resistive load

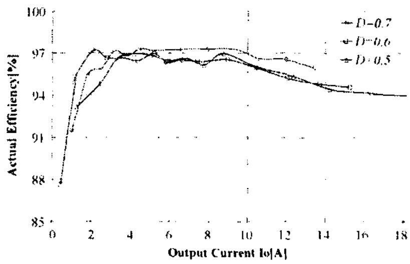

Fig. 15 Actual efficiency vs. load current I_0

Fig. 15 demonstrates actual efficiency as a function of the output current Io with different value of the duty cycle D. The actual efficiency over 94[%] is obtained over the wide load variation range and duty cycle changes.

ACKNOWLEDGMENT

This work was supported by the Korea Research Foundation Grant funded by the Korean Government (MOEHRD) (KRF-2005-037- D00006)

4. Conclusion

In this paper, a new a new full-bridge soft-switching phase shift PWM DC-DC Converter has been proposed, which is suitable for fuel cell based power generation system. The proposed converter has outstanding advantage over the conventional DC-DC converter with respect to high efficiency, high power density, and high component utilization. In special, the proposed converter has predominant high boosting output voltage and high efficiency characteristics under the inherently severs low output voltage of the fuel cell through the overall load conditions. Moreover, the developed converter has been experimentally tested with the help of a fuel cell simulator, and can generate the V-I characteristics of proton exchange membrane(PEM) fuel cell, so that the performance of the proposed converter could be effectively examined and the validity of the converter could be verified.

REFERENCES

[1] Eun-Soo Kim, Yoon-Ho Kim, "An improved soft-switching PWM FB DC/DC converter for reducing conduction losses", IEEE Trans. on PE, Vol.14, No.2, pp.258-263, 1999.

[2] J.G.Cho, "Novel Zero-Voltage and zero-current-switching Full Bridge PWM Converter Using Transformer Auxiliary Winding", IEEE Trans. on PE, Vol.15, No.2, pp.250-257, 2000.

[3] National Oceanic and Atmospheric Administration: Climate of 2001, Annual Review.

[4] S.Moisseev, "High-Frequency Forward Transformer Linked PWM DC-DC Power Converter with Zero Voltage Switching and Zero Current Switching Bridge Legs", KIPE-Journal of Power Electr -onics, Vol.2 No.4, pp.278-287, 2002.

[5] S. Moisseev, S. Hamada, M. Nakaoka, "Innovative Proposal of Full-Bridge Phase-Shift PWM DC-DC Converter with ZVS and ZCS Bridge Legs using Tapped Inductor" IEEE International Telecommunications Energy Conference, pp.778-783, 2003

[6] National Oceanic and Atmospheric Administration: Climate of 2001, Annual Review.

[7] T. Shinoki, M. Matsumura, and A. Sasaki, "Development of an internal reforming molten carbonate fuel cell stack," IEEE Trans. Energy Conv., vol. 10, no. 4, pp. 722-729, Dec. 1995.